

International Atomic Energy Agency

INDC(CCP)-280/L

INDC

INTERNATIONAL NUCLEAR DATA COMMITTEE

TRANSLATION OF SELECTED PAPERS PUBLISHED
IN NUCLEAR CONSTANTS, No. 2, Moscow 1987

(Original Report in Russian was distributed
as INDC(CCP)-277/G)

Translated by the IAEA

January 1988

IAEA NUCLEAR DATA SECTION, WAGRAMERSTRASSE 5, A-1400 VIENNA

TRANSLATION OF SELECTED PAPERS PUBLISHED
IN NUCLEAR CONSTANTS, No. 2, Moscow 1987

(Original Report in Russian was distributed
as INDC(CCP)-277/G)

Translated by the IAEA

January 1988

**Reproduced by the IAEA in Austria
January 1988**

88-00351

Table of Contents

Evaluation of ^{236}U Neutron Data in the Resolved and Unresolved Resonance Energy Region A.B. Klepatskij, V.A. Kon'shin, Yu.V. Porodzinskij, E.Sh. Sukhovitskij 5
Measurement of the Neutron Radiative Capture Cross- Sections for Silver in the Energy Region 4-400 keV M.V. Bokhovko, L.E. Kazakov, V.N. Kononov, E.E. Poletaev, V.M. Timokhov, A.A. Voevodskij 15

Abstract

Evaluation of ^{236}U neutron data in the fast neutron energy region. Theoretical models which had been tested against experimental data available for ^{238}U , ^{235}U , ^{239}Pu were used for ^{236}U neutron cross section evaluation and theoretical prediction. The up-to-date analysis seems to lead to more reliable data for inelastic scattering excitation functions, $(n,2n)$, $(n,3n)$ -cross-sections, angular distributions of elastically and inelastically scattered neutrons, total, inelastic and elastic cross-sections for which experimental data are not available.

EVALUATION OF ^{236}U NEUTRON DATA IN THE RESOLVED AND
UNRESOLVED RESONANCE ENERGY REGION

A.B. Klepatskij, V.A. Kon'shin, Yu.V. Porodzinskij,
E.Sh. Sukhovitskij

The need to obtain a more accurate knowledge of ^{236}U nuclear data is a result of the fact that when spent uranium (regenerate) is re-used in nuclear fuel, the content of ^{236}U increases significantly and, since it is a nuclear poison, it impairs the utilization of neutrons in the reactor [1]. In order to compensate for the harmful effect of this isotope, the initial concentration of ^{235}U in the regenerated fuel has to be increased. The amount of ^{235}U which needs to be added depends on the amount of ^{236}U in the regenerate and on the design of the fuel elements. The accumulation of ^{236}U may be fairly significant (about 0.5%) if the residual ^{235}U enrichment in the fuel is less than 1% (in WWER-type reactors). Therefore, during reactor operation, the reactivity effect dependent on ^{236}U has to be taken into account. Furthermore, ^{232}U is formed in the fuel from ^{236}U .

This paper examines the ^{236}U neutron cross-sections in the thermal region and the resolved and unresolved resonance regions.

Most of the experimental data on neutron cross-sections in the resolved resonance region is unavailable in numerical form and therefore the evaluation for this region was based on the resonance parameters given in Refs [2-8]. Data on the measurement of the absorption cross-section σ_a ^{236}U [5, 9-12] and total cross-section σ_t [7] at the maximum value of the thermal neutron spectrum are shown in Table 1. The experimental data for ^{236}U capture resonance integrals (at 10^{-28} m^3) are given below:

[9]	381 ± 20
[10]	397 ± 34
[11]	450 ± 30
[12]	340 ± 15
Our evaluation	330 ± 33.

Table 1. Experimental and evaluated cross-sections for ^{236}U at the maximum value of the thermal neutron spectrum, 10^{-28} m^2

Reference	σ_t	σ_a
[7]	$18,7 \pm 1,7$	-
[9]	-	$5,0 \pm 2,0$
[10]	-	$5,5 \pm 0,3$
[11]	-	$6,0 \pm 1,0$
[5]	-	$5,10 \pm 0,25$
[12]	-	$5,00 \pm 0,14$
Our evaluation	$18,58 \pm 1,50$	$5,07 \pm 0,15$

Note: In this work $\sigma_n = 13.51 \pm 1.0$.

The experimental values of the resonance parameters [2-8] are generally not at variance with one other. The positions of resonances in the energy region up to 415 eV were determined from the data in Ref. [5] and in the higher region from the data in Refs [3 and 4]. The resonance neutron widths were obtained by averaging, taking into account the errors in the experimental data. We redetermined the radiation widths from the evaluated neutron widths so as to preserve the area under each of the capture resonances, i.e. so that $\Gamma_{\gamma i} \Gamma_{n i} / \Gamma_{t i} = \text{const}$. The fission widths from Ref. [8] were taken for those resonances for which they were measured.

The energy and width of the first resonance were varied within the limits of error in order to describe - taking into account the negative resonance - the experimental data in the region up to the first resonance and our evaluation of the radiative capture cross-section at 0.0253 eV, which was $5.0 \times 10^{-28} \text{ m}^2$.

The evaluated resonance parameters of ^{236}U are given in Table 2. The neutron cross-sections in the resolved resonance region ($10^{-5} \text{ eV} - 1 \text{ keV}$) were calculated from the multi-level Breit-Wigner formula covering the contribution of all levels. The potential scattering cross-section obtained from calculations using the coupled channel method and agreement with experimental data on the total cross-section in the thermal region was

Table 2. Evaluated resonance parameters for ^{236}U

E_i , eV	Γ_{n_i} , MeV	Γ_d , MeV	Γ_f , MeV	E_i , eV	Γ_{n_i} , MeV	Γ_d , MeV	Γ_f , MeV
-4,54	8,406	2,0594	0,035	563,8	80,25	21,98	0,354
5,49	2,10	25,0	0,29	576,2	144,21	25,93	0,354
29,7	0,587	22,77	0,16	607,1	13,27	20,07	0,354
34,0	2,36	20,14	0,18	617,8	52,34	23,93	0,354
43,7	14,09	17,76	0,43	637,8	76,00	24,20	0,354
63,1	0,037	22,77	0,354	647,6	6,10	22,77	0,354
71,1	18,73	23,36	0,29	655,6	97,95	22,89	0,354
86,0	28,56	21,43	0,30	673,6	56,02	23,72	0,354
101,7	0,88	22,77	0,354	691,3	32,35	26,76	0,354
120,2	50,81	22,01	0,34	706,0	28,89	20,90	0,354
124,2	16,71	19,52	0,21	720,6	97,66	20,97	0,354
133,7	1,20	22,77	0,354	746,25	20,76	17,73	0,354
137,0	0,57	22,77	0,354	770,65	185,22	21,94	0,354
163,7	2,10	22,77	0,354	789,4	85,46	22,97	0,354
192,6	9,01	22,77	0,354	806,6	38,83	23,91	0,354
194,0	45,41	19,07	0,500	820,3	8,96	22,77	0,354
212,0	87,65	24,25	0,320	827,4	240,03	27,96	0,354
229,0	2,01	22,77	0,354	849,0	3,00	22,77	0,354
243,0	0,30	22,77	0,354	864,9	17,03	18,96	0,354
272,4	31,58	24,45	0,400	888,8	7,75	22,77	0,354
288,2	12,77	20,56	0,480	900,35	4,86	22,77	0,354
302,5	77,67	23,72	0,460	930,7	7,54	22,77	0,354
320,0	5,41	22,77	0,354	948,4	163,10	23,98	0,354
334,4	6,22	22,77	0,354	955,2	37,50	22,77	0,354
356,0	0,70	22,77	0,354	969,3	309,05	22,95	0,354
367,8	0,40	22,77	0,354	994,7	151,83	21,96	0,354
371,0	14,23	21,99	0,42	998,1	11,00	22,77	0,354
379,3	92,54	22,78	0,30	1013,1	15,38	22,77	0,354
415,0	15,87	21,67	0,59	1024,2	245,61	26,40	0,354
430,9	60,44	21,94	0,354	1032,1	37,47	23,30	0,354
440,6	62,43	23,94	0,354	1064,6	36,10	28,29	0,354
465,5	14,06	21,61	0,354	1075,7	9,00	22,77	0,354
478,4	37,92	20,71	0,354	1084,2	2,00	22,77	0,354
500,4	2,47	22,77	0,354	1098,0	3,00	22,77	0,354
507,1	19,10	21,87	0,354	1104,7	123,30	24,95	0,354
536,4	31,50	21,26	0,354	1132,1	11,43	22,77	0,354
542,9	10,40	29,18	0,354				

$11.4 \times 10^{-28} \text{ m}^2$. The evaluated cross-sections in the 10^{-5} -10 eV energy range are given in Table 3.

In the region up to 1132.1 keV, 72 resonances have been found experimentally (see Table 2), which give the values $\langle D \rangle = 15.87 \text{ eV}$ and $\langle \Gamma_n^0 \rangle = 1.88 \text{ MeV}^{1/2}$. A correction has to be made to these values for the missed levels owing to the narrowness of the neutron widths and the presence of multiplets. The omissions were taken into account using the methods developed in Refs [13 and 14]. The methods described in the

Table 3. Evaluated neutron cross-sections for ^{236}U (in 10^{-28} m^2) in the energy region 10^{-5} -10 eV at zero temperature

$E, \text{ eV}$	σ_{np}	σ_n	σ_f	$E, \text{ eV}$	σ_{np}	σ_n	σ_f
10^{-5}	250,960	13,548	3,423	5,1	42,821	2,323	0,497
$2 \cdot 10^{-5}$	177,455	13,548	2,241	5,2	76,579	0,776	0,889
$4 \cdot 10^{-5}$	125,480	13,548	1,712	5,30	176,125	0,221	2,043
10^{-4}	79,361	13,548	1,082	5,35	321,434	3,306	3,729
$2 \cdot 10^{-4}$	56,117	13,548	0,765	5,40	763,851	21,716	8,861
$4 \cdot 10^{-4}$	39,681	13,548	0,541	5,43	1666,714	72,879	19,334
10^{-3}	25,098	13,547	0,342	5,46	5788,496	360,945	67,147
$2 \cdot 10^{-3}$	17,748	13,546	0,242	5,49	33472,370	2822,987	388,279
$4 \cdot 10^{-3}$	12,552	13,543	0,171	5,52	5756,426	631,421	66,775
10^{-2}	7,943	13,534	0,108	5,55	1648,510	228,203	19,123
$2 \cdot 10^{-2}$	5,621	13,520	0,077	5,58	751,386	128,170	8,716
0,0253	5,000	13,512	0,068	5,65	240,014	62,147	2,784
$5 \cdot 10^{-2}$	3,565	13,477	0,049	5,70	139,159	46,420	1,614
0,1	2,533	13,407	0,034	5,80	63,476	32,501	0,737
0,2	1,811	13,271	0,024	5,90	36,028	26,293	0,418
0,5	1,200	12,888	0,016	6,00	23,114	22,823	0,268
1,0	0,952	12,318	0,012	6,20	11,756	19,092	0,137
1,5	0,914	11,803	0,011	6,40	7,061	17,122	0,082
2,0	0,977	11,313	0,012	6,60	4,686	15,900	0,055
2,5	1,141	10,816	0,014	6,80	3,325	15,063	0,039
3,0	1,454	10,273	0,017	7,00	2,476	14,451	0,029
3,5	2,058	9,616	0,024	7,50	1,365	13,446	0,016
4,0	3,378	8,708	0,039	8,00	0,860	12,624	0,010
4,2	4,373	8,209	0,051	8,50	0,590	12,390	0,007
4,4	5,959	7,573	0,069	9,00	0,429	12,064	0,005
4,6	8,712	6,722	0,101	9,50	0,327	11,806	0,004
4,8	14,149	5,508	0,164	10,00	0,258	11,594	0,003
5,0	27,427	3,641	0,318				

literature for introducing corrections for the level omissions are based on the Porter-Thomas distribution for neutron widths . The authors of these methods determine in different ways the distortion of the Porter-Thomas distribution caused by the level gap. In this case, the level spacing distribution is not used and no attempts are made to determine the distortion of the Wigner distribution. In Ref. [14] both distributions are used simultaneously, based on the proposed model probability function for the level gap resulting in distortion of the theoretical neutron width distributions and level spacing. Then, by comparing the theoretical and experimental distributions using the maximum likelihood method, the parameters of the model level gap probability function are determined and hence the mean neutron widths and level spacing.

Application of the method in Ref. [13] to the analysis of resonance parameters in the energy region up to 1132.1 eV has shown that the mean values of $\langle D \rangle$ and $\langle \Gamma_n^0 \rangle$ are 15.1 ± 0.5 eV and $(1.76 \pm 0.20) \text{ MeV}^{1/2}$ respectively, and $\langle S_0 \rangle = (1.16 \pm 0.20) \times 10^{-4} \text{ eV}^{-1/2}$. The calculations made by the method in Ref. [14] have shown that the mean spacing $\langle D \rangle$ is approximately 7% lower than that obtained by other methods ($\langle D \rangle = 14.13 \pm 0.50$ eV), $\langle \Gamma_n^0 \rangle = 1.634 \pm 0.250 \text{ MeV}^{1/2}$, $\langle S_0 \rangle = (1.16 \pm 0.18) \times 10^{-4} \text{ eV}^{-1/2}$. It is obvious that if both distributions (Porter-Thomas and Wigner) are taken into account, it is possible to determine the experimental conditions more precisely and to make more accurate corrections for level omission.

If it is assumed that only S-resonances are present, the evaluations of the mean resonance parameters are: $\langle D \rangle = 14.1 \pm 0.5$ eV, $\langle \Gamma_n^0 \rangle = 1.63 \pm 0.25 \text{ MeV}^{1/2}$, $\langle S_0 \rangle = (1.16 \pm 0.18) \times 10^{-4} \text{ eV}^{-1/2}$, $\langle \Gamma_\gamma \rangle = 22.77 \pm 1.30 \text{ MeV}$, and $\langle \Gamma_f \rangle = 0.354 \pm 0.100 \text{ MeV}$.

In the unresolved resonance energy region (1-150 keV), experimental data are available only for the cross-sections $\sigma_{n\gamma}$ [5, 15-19] and σ_t [20 and 21], and are not available for σ_t , σ_n , σ_{nn} . In order to obtain the mean parameters, the method recommended in the ENDF/B format was used.

The mean level spacings $\langle D \rangle_j$ were determined from $\langle D \rangle$ in the resolved resonance region using the level density from the superfluid nuclear model, taking into account the vibrational and rotating modes [22]. If the energy dependence at 1 and 150 keV is taken into account, then $D_{1/2}$ is 14.1 and 10.5 eV respectively, $D_{3/2}$ is 7.33 and 5.44 eV, and $D_{5/2}$ is 5.21 and 3.86 eV. The mean neutron widths were calculated using the strength functions S_λ . In the ground state, S_0^{0+} was taken to be equal to that evaluated from the resolved resonance region: $1.156 \times 10^{-4} \text{ eV}^{-1/2}$. Calculations using the coupled channel method gave $S_0^{0+} = 1.164 \times 10^{-4} \text{ eV}^{-1/2}$ and $S_1^{0+} = 1.74 \times 10^{-4} \text{ eV}^{-1/2}$.

Since the resonance structure in the fission widths of resolved resonances has not been shown experimentally, the mean fission widths $\langle \Gamma_f \rangle$ were calculated with the single peak approximation using the Hill-Wheeler

model. The parameters of the fission barrier in the $1/2^+$ channel were selected so that the mean width $\langle \Gamma_f \rangle_{1/2^+}$ calculated in the 1 keV region was equal to the average from the resolved resonance region (0.356 MeV at 1 keV and 0.854 MeV at 150 keV). The height of the barrier in this case was $E_f^{1/2^+} = 6.328$ MeV with the assumption of the curvature parameter $\hbar\omega = 0.8$ MeV (as follows from systematics).

The parameters of the fission barriers for other states were selected so as to describe the experimental data [20 and 21] and to make a smooth 'seam' with the fission cross-section in the fast energy region. Here it proved necessary to introduce the following increases above the fission threshold for the $1/2^+$ state: $\Delta E_f^{1/2^-} = 0.300$ MeV, $\Delta E_f^{3/2^+} = 0.382$ MeV, $\Delta E_f^{5/2^+} = 0.250$ MeV. The mean fission widths for energies of 1 and 150 keV were respectively $\langle \Gamma_f \rangle_{1/2^-} = 0.034$ and 0.081 MeV, $\langle \Gamma_f \rangle_{3/2^+} = 0.018$ and 0.044 MeV, and $\langle \Gamma_f \rangle_{5/2^+} = 0.056$ and 0.133 MeV.

The energy dependence of the mean radiation widths in the energy region studied was taken into account (at 1 keV $\langle \Gamma_\gamma \rangle$ is 22.77 MeV, at 150 keV it is 24.20 MeV). Since the dependence of $\langle \Gamma_\gamma \rangle$ on the channel spin (if there is no level density dependence on parity) predicted from the γ -quanta cascade-emission model is much smaller than the experimental error $\Delta \overline{\Gamma}_\gamma$ determined in the resolved resonance region, the width $\langle \Gamma_\gamma \rangle$ is assumed to be independent of state spin.

The calculations of the mean resonance parameters were taken up to the level 6^+ excitation threshold (about 300 keV), allowing for the competition of inelastic scattering at level 4^+ . Here the difference in the strength functions for the ground and excited states was taken into account and calculated using the generalized optical method [23]. These strength functions were:

$$S_{0-1/2}^{2+} = 1.0 \times 10^{-4} \text{ eV}^{-1/2}, \quad S_1^{2+} = 1.54 \times 10^{-4} \text{ eV}^{-1/2},$$

$$S_0^{4+} = 0.78 \times 10^{-4} \text{ eV}^{-1/2}, \quad S_1^{4+} = 3.0 \times 10^{-4} \text{ eV}^{-1/2}.$$

A comparison of the evaluated and experimental values for the radiative capture cross-sections is shown in Fig. 1. As can be seen, there is good

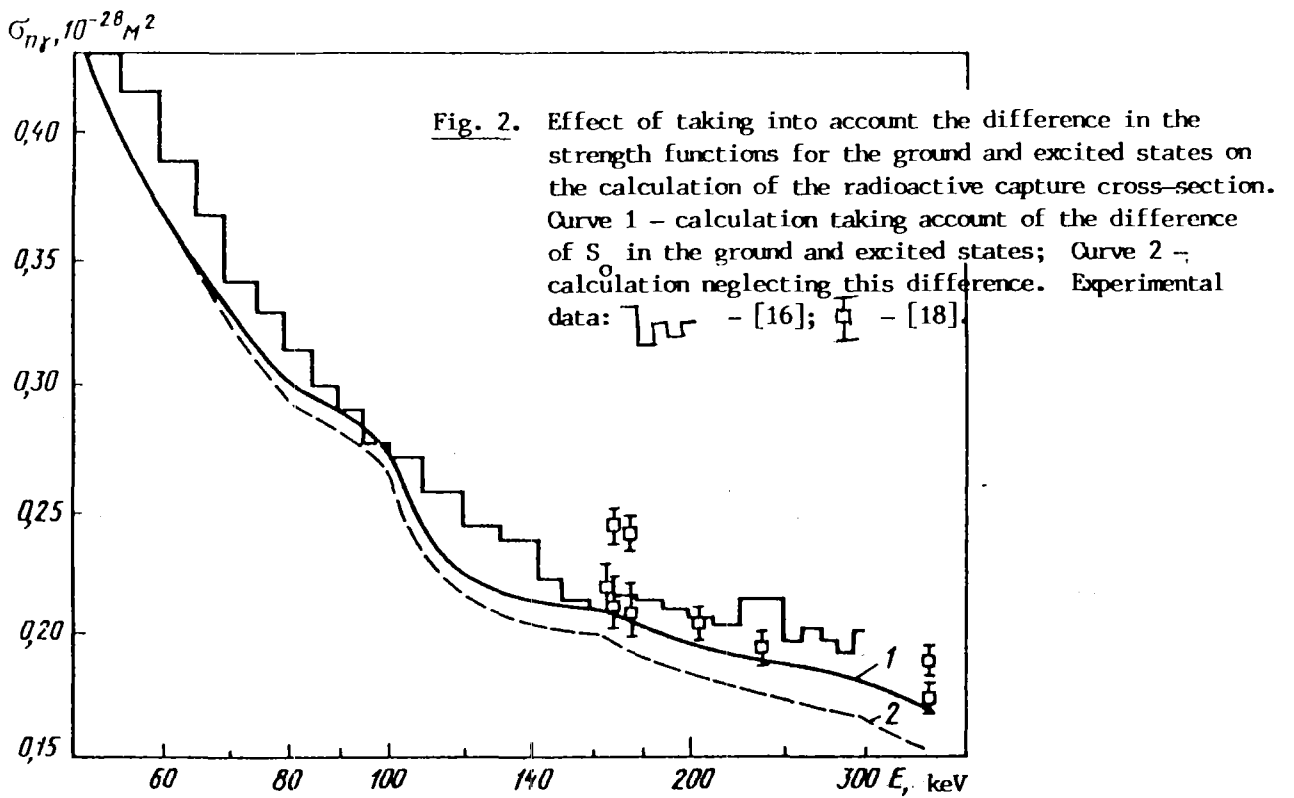
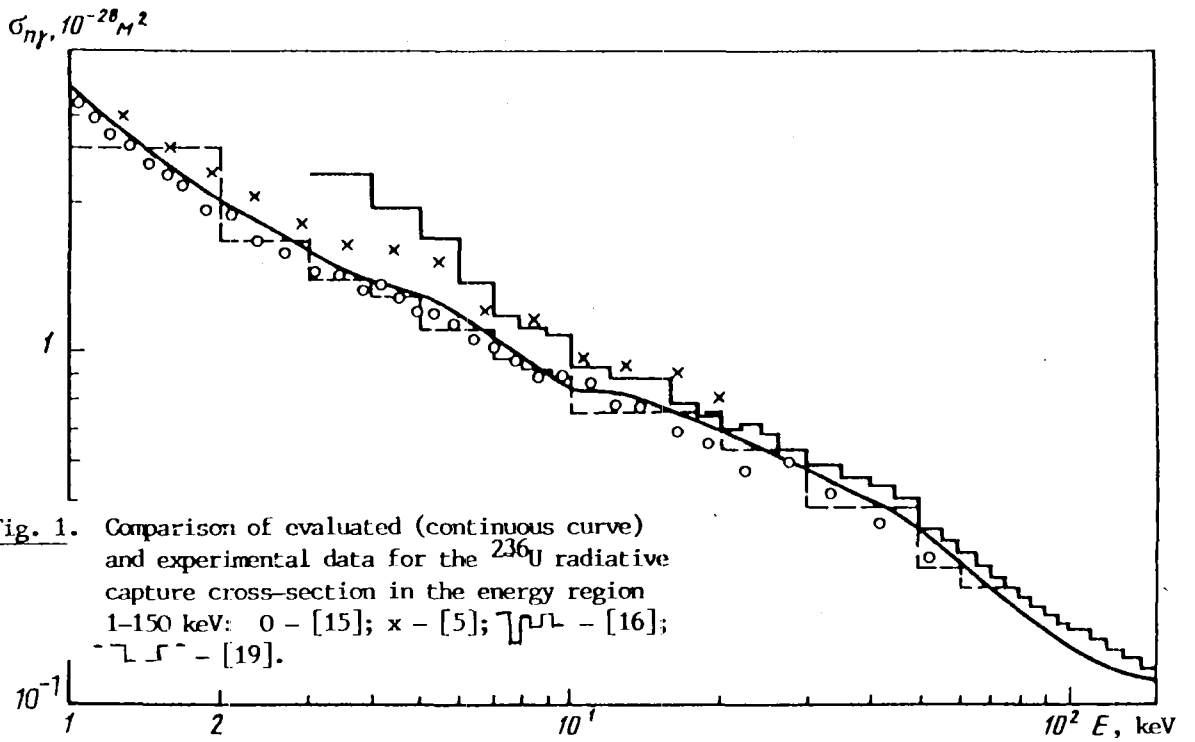


Table 4. Mean neutron cross-sections in the unresolved resonance energy region, 10^{-28} m^2

E, keV	σ_t	σ_n	$\sigma_{nn'}$	σ_f	σ_{nf}
1,0	26,564	23,202	0,0	0,049	3,313
1,5	23,809	21,272	-	0,035	2,502
2,0	22,170	20,067	-	0,028	2,075
2,5	21,052	19,283	-	0,022	1,747
3	20,227	18,633	-	0,020	1,574
4	19,070	17,696	-	0,016	1,358
6	17,696	16,596	-	0,011	1,069
8	16,874	15,909	-	0,009	0,956
10	16,311	15,417	-	0,008	0,886
12	15,890	15,071	-	0,006	0,813
14	15,561	14,768	-	0,006	0,787
16	15,293	14,527	-	0,006	0,760
20	14,876	14,181	-	0,005	0,690
24	14,559	13,921	-	0,004	0,634
28	14,304	13,721	-	0,004	0,579
32	14,093	13,545	-	0,003	0,545
36	13,913	13,389	-	0,003	0,521
40	13,756	13,257	-	0,003	0,496
45	13,584	13,100	0,0	0,003	0,481
50	13,428	12,959	0,038	0,003	0,428
60	13,184	12,666	0,146	0,002	0,370
70	12,980	12,404	0,240	0,002	0,334
80	12,819	12,184	0,332	0,002	0,301
90	12,676	11,990	0,414	0,002	0,270
100	12,578	11,828	0,495	0,002	0,253
110	12,473	11,661	0,573	0,002	0,237
120	12,373	11,513	0,632	0,002	0,226
130	12,270	11,367	0,681	0,002	0,220
140	12,171	11,240	0,717	0,002	0,212
150	12,076	11,114	0,748	0,002	0,212

agreement between the evaluated and the experimental values [19]. In the region up to 10 keV our calculations virtually coincide with those of Refs [15 and 19], in the region 10-50 keV they coincide with those of Ref. [19] and lie between those of Refs [15 and 16]. In the region 50-160 keV the evaluation is somewhat lower than the data in Ref. [16] (almost within the limits of experimental error) and coincides with the results of Refs [17 and 18]. As the calculations have shown, it is impossible to describe the experimental data with single parameters for the whole energy region 1-300 keV unless the difference between the strength functions of the ground and excited states is taken into account. Figure 2 shows that the calculation of the dependence of $\sigma_{ny}(E)$ on the strength functions of the ground and the excited states,

is lower than the experimental data for the energy region above the (n,n') reaction threshold.

The cross-sections σ_t , σ_n , $\sigma_{nn'}$, for which no experimental data are available, were predicted theoretically from the evaluated mean parameters and calculations. The inelastic scattering cross-section $\sigma_{nn'}$ was calculated taking into account the contribution of the direct process. Values for the evaluated neutron cross-sections in the 1-150 keV region are shown in Table 4.

From what has been said, it is possible to draw the following conclusions:

1. Evaluation of the neutron cross-sections of ^{236}U makes it possible to obtain evaluated resonance parameters describing all the available experimental data in the thermal and resonance energy regions; in the unresolved resonance region (1-150 keV) the cross-sections σ_t , σ_n , $\sigma_{nn'}$ for which there are no experimental data, are predicted theoretically;
2. It proved possible to describe the experimental data for the radiative capture cross-section with single parameters for the whole energy region studied, if the difference between the strength functions for the ground and the excited states was taken into account;
3. The degree of reliability of the corrections made for the level gap remains an open question, since the present methods give values of $\langle D \rangle$ which differ by about 10%.

MEASUREMENT OF THE NEUTRON RADIATIVE CAPTURE CROSS-SECTIONS FOR SILVER
IN THE ENERGY REGION 4-400 keV

M.V. Bokhovko, L.E. Kazakov, V.N. Kononov, E.E. Poletaev,
V.M. Timokhov, A.A. Voevodskij

The paper contains the results of neutron radiative capture cross-section measurements in the 4-400 keV energy region for the isotopes ^{107}Ag and ^{109}Ag and their natural mixture $_{47}\text{Ag}$. Radiative capture is among the basic processes determining the neutron balance in nuclear reactors. The isotope ^{109}Ag is one of the common fission products; accurate knowledge of its neutron capture cross-section is important for fast reactor calculations, particularly in the case of high nuclear fuel burnup values. The averaged fast neutron radiative capture cross-section for silver isotopes also provides information about the neutron and radiative strength functions for s- and p- neutrons, since the silver nuclei lie in the region of the maximum of the p- wave neutron strength function.

The radiative capture cross-section measurements in the 4-400 keV energy region for the isotopes ^{107}Ag and ^{109}Ag and their natural mixture were made using a fast and resonance neutron spectrometer based on the pulsed Van de Graaff EhG-1 accelerator at the Institute of Physics and Energetics [1]. In order to obtain neutrons with a continuous spectrum, the $^7\text{Li}(p,n)^7\text{Be}$ reaction was used together with a "thick" target of metallic lithium. The cross-sections were measured by the method based on the recording of prompt capture γ -quanta and using the time-of-flight technique to determine the neutron energy and background discrimination. The prompt capture gammas were recorded by a spherical scintillator with a 17-L tank to which 60% trimethylborate was added to reduce the sensitivity to scattered neutrons. The relative flux of neutrons impinging on the sample was measured by a detector with a thin (1 mm) NE-912-grade ^6Li -glass positioned in front of the sample and the detector. The latter consisted of a ^{10}B -plate and two NaI(Tl) crystals and was situated behind the sample.

In the experiment we used samples of the separated isotopes with an enrichment of 98.9% (^{107}Ag) and 99.4% (^{109}Ag) in the form of metal powder, and natural silver in the form of 0.2 mm-thick metal foil. The thickness of the samples was about 1.3×10^{-2} atom/b. The measurements in the 2-130 keV energy region were made over a flight path of 0.72 m with a 7 mm-thick ^{23}Na filter permanently located in the neutron beam. This filter made it possible to determine the background in the 2.85 keV resonance region and to calibrate the energy scale for the 53.191 keV resonance. The measurements in the 16-500 keV energy range were made over a flight path of 2.4 m. The same flight path was used for measurements in the electronvolt energy region (2-20 eV) which are necessary for standardizing the cross-sections using the saturated resonance method. For this purpose the target was surrounded by a polyethylene moderator, the dimensions of which were selected so as to ensure an optimum ratio between the resonance neutron yield and the spectrometer resolution. Neutrons with an energy of less than 2 eV which under our experimental conditions were released with a repeated cycle were absorbed by cadmium (thickness 1.6 mm) and indium (thickness 8 mm) filters. Use of the indium filter also made it possible to measure the background of the detectors for strong indium resonance regions at neutron energies of 3.86 and 9.12 eV. A detailed description of the spectrometer, the measurement methods and the processing of the results is contained in Ref. [2].

In order to make the cross-section measurements absolute, the saturated resonance method was used in conjunction with the pulse-height weighting technique, which made it possible to reduce significantly the sensitivity to measurements in the spectrum and the multiplicity of the γ -quanta from capture events on transition from the neutron energy resonance region to the fast neutron region and from nucleus to nucleus.

In the case of ^{107}Ag and ^{109}Ag , standardization was performed using the mean standardizing coefficient which was derived from measurements in the resonance region using the pulse-height weighting technique for nuclei with

Table Neutron radiative capture cross-sections for ^{107}Ag , ^{109}Ag
and ^{47}Ag , mb

E, keV	^{107}Ag	^{109}Ag	^{47}Ag	E, keV	^{107}Ag	^{109}Ag	^{47}Ag
4-5	1809 \pm 150	1677 \pm 149	1771 \pm 191	84-88	502 \pm 27	469 \pm 21	477 \pm 26
5-6	1474 \pm 106	1561 \pm 106	1668 \pm 138	88-92	492 \pm 27	474 \pm 21	474 \pm 26
6-7	1402 \pm 81	1513 \pm 88	1420 \pm 108	92-96	471 \pm 25	453 \pm 20	458 \pm 25
7-8	1304 \pm 74	1309 \pm 68	1372 \pm 93	96-100	459 \pm 25	432 \pm 19	443 \pm 24
8-9	1346 \pm 75	1512 \pm 73	1400 \pm 87	100-110	448 \pm 24	437 \pm 20	435 \pm 23
9-10	1299 \pm 71	1418 \pm 67	1392 \pm 84	110-120	418 \pm 23	394 \pm 18	394 \pm 22
10-12	1206 \pm 65	1274 \pm 57	1234 \pm 72	120-130	405 \pm 22	380 \pm 17	373 \pm 21
12-14	1136 \pm 61	1128 \pm 50	1139 \pm 64	130-140	390 \pm 21	378 \pm 17	367 \pm 20
14-16	1070 \pm 58	993 \pm 44	1035 \pm 58	140-150	373 \pm 20	350 \pm 16	352 \pm 19
16-18	1080 \pm 58	1067 \pm 46	1077 \pm 59	150-160	363 \pm 20	336 \pm 15	332 \pm 18
18-20	1060 \pm 56	1031 \pm 44	1036 \pm 56	160-170	347 \pm 19	325 \pm 15	322 \pm 18
20-22	972 \pm 52	1019 \pm 45	973 \pm 54	170-180	339 \pm 18	317 \pm 14	320 \pm 18
22-24	947 \pm 51	1008 \pm 44	967 \pm 53	180-190	320 \pm 17	306 \pm 14	305 \pm 17
24-26	920 \pm 50	907 \pm 40	917 \pm 50	190-200	326 \pm 18	307 \pm 14	306 \pm 17
26-28	891 \pm 48	848 \pm 38	866 \pm 48	200-210	303 \pm 17	298 \pm 13	306 \pm 17
28-32	824 \pm 44	833 \pm 37	822 \pm 45	210-220	300 \pm 17	290 \pm 13	281 \pm 16
32-36	840 \pm 45	797 \pm 36	811 \pm 45	220-230	301 \pm 17	284 \pm 13	286 \pm 16
36-40	741 \pm 40	749 \pm 34	738 \pm 41	230-240	302 \pm 17	284 \pm 13	273 \pm 16
40-44	695 \pm 38	710 \pm 32	692 \pm 38	240-250	286 \pm 16	177 \pm 12	263 \pm 15
44-48	708 \pm 38	663 \pm 30	685 \pm 38	250-260	280 \pm 16	277 \pm 13	264 \pm 15
48-52	660 \pm 36	643 \pm 29	638 \pm 35	260-270	275 \pm 16	268 \pm 12	270 \pm 16
52-56	605 \pm 33	595 \pm 27	582 \pm 32	270-280	282 \pm 16	267 \pm 13	268 \pm 16
56-60	603 \pm 33	606 \pm 27	589 \pm 32	280-290	278 \pm 16	258 \pm 12	254 \pm 15
60-64	595 \pm 32	584 \pm 26	568 \pm 31	290-300	279 \pm 16	259 \pm 12	255 \pm 15
64-68	572 \pm 31	546 \pm 25	542 \pm 30	300-320	268 \pm 15	259 \pm 12	241 \pm 14
68-72	561 \pm 30	533 \pm 24	540 \pm 30	320-340	247 \pm 10	225 \pm 10	221 \pm 13
72-76	555 \pm 30	527 \pm 24	527 \pm 29	340-360	224 \pm 13	205 \pm 9	209 \pm 12
76-80	535 \pm 29	510 \pm 23	507 \pm 28	360-380	213 \pm 12	196 \pm 9	198 \pm 11
80-84	503 \pm 27	477 \pm 21	478 \pm 26	380-400	198 \pm 11	179 \pm 8	185 \pm 10

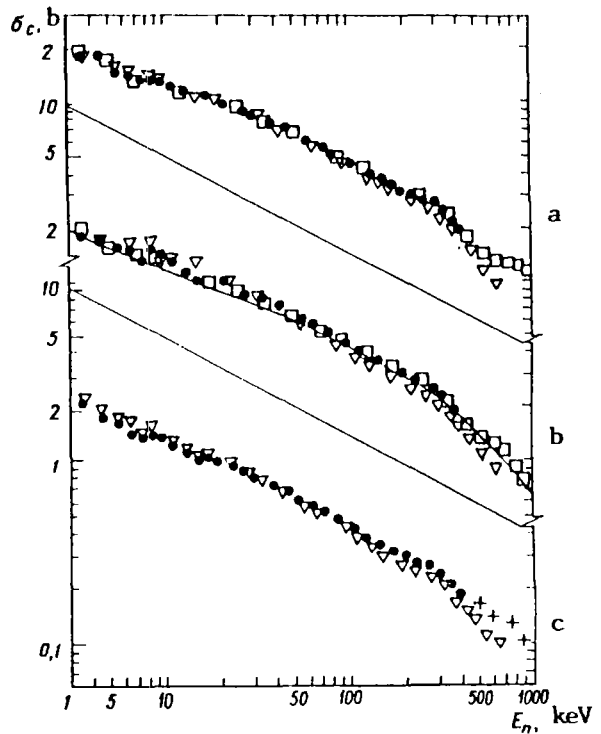
saturated resonances (^{197}Au , ^{109}Ag , ^{181}Ta , ^{182}W , ^{145}Nd) [3]. The cross-section for the ^{109}Ag isotope was standardized from its own saturated resonance with $E_0 = 5.19$ eV. Correction for multiple scattering and self-shielding in the samples studied in the fast neutron region was made algorithmically as described in Ref. [4]. Corrections for self-absorption of γ -quanta in the samples were calculated by the Monte-Carlo method using the model spectra of capture events and real geometrical conditions [5]. In order to obtain the dependence $\sigma_c(E)$ for energies up to 130 keV, the relative dependence of the $^6\text{Li}(n,\alpha)^3\text{H}$ reaction cross-section was used. For higher energies, the $^{10}\text{B}(n,\alpha\gamma)^7\text{Li}$ reaction was used to measure the shape of the neutron flux, and the data were standardized to the cross-section

values obtained in the 50-110 keV range. The cross-sections of the reference reactions ${}^6\text{Li}(n,\alpha){}^3\text{H}$ and ${}^{10}\text{B}(n,\alpha,\gamma){}^7\text{Li}$ were taken from the evaluation in the ENDF/B-V library. Corrections for multiple neutron scattering in the neutron flux detectors were calculated by the Monte-Carlo method. The magnitude of the error in the results obtained was governed by the statistical accuracy of the measurements and the systematic errors of the method. The statistical error was about 1% at 30-400 keV and increased to 10% at 4 keV. The error associated with deducting background was 6-9% at 4 keV and less than 1% at energies above 30 keV. The error in the relative dependence of the ${}^6\text{Li}(n,\alpha){}^3\text{H}$ reaction cross-section was taken to be 0.5-2%, and for the ${}^{10}\text{B}(n,\alpha,\gamma){}^7\text{Li}$ reaction about 3% [6]. The accuracy of the corrections for the final thickness of the sample was determined mainly from the accuracy of the parameters used and estimated at 3%. The error in the standardization coefficient for ${}^{107}\text{Ag}$ and ${}_{47}\text{Ag}$ was estimated to be 4% and for ${}^{109}\text{Ag}$ 2.5%.

The results of the neutron radiative capture cross-sections for the nuclei ${}^{107}\text{Ag}$, ${}^{109}\text{Ag}$ and ${}_{47}\text{Ag}$ and their total error are shown in the table and figure. The figure also shows the results of the experimental work and evaluations made during recent years. Examination of the data shows that the neutron capture cross-sections for ${}^{107}\text{Ag}$ and ${}^{109}\text{Ag}$ obtained in this paper agree well with the results of Ref. [7] over the whole energy range. The data of the Japanese group [8] also agree satisfactorily with the results of our work in the energy region up to 100 keV, while for higher neutron energies they are systematically 7-10% lower for both isotopes. Both silver isotopes at an excitation energy of about 300 keV have the 3/2-level exhibiting high excitation during inelastic neutron scattering, which appears in the radiative capture cross-section in the form of a characteristic break in the energy dependence of the cross-section observed in all the latest works. For the natural isotope mixture in the 20-100 keV energy region, our data are in good agreement with the results of Ref. [8]. However, for neutron

Figure.

Radiative capture cross-sections for ^{107}Ag (a), ^{109}Ag (b) and ^{47}Ag (c) based on data from \square - [7]; ∇ - [8]; $+$ - [9]; — - [10]; \bullet - the present paper.



energies above 100 keV, the data of Ref. [8] are systematically lower than ours by about 10%. It should be noted that the capture cross-section for the natural mixture, obtained by summing the contribution of the cross-sections measured experimentally in the present paper for the separate isotopes, agrees to within 1-2% with the experimental data obtained for the natural silver sample. Similar comparison of the data from Ref. [8] shows a discrepancy in the energy dependence of the calculated and measured cross-sections amounting to 15% of the absolute value at the limits of the range. This demonstrates the poor consistency of the results in Ref. [8]. It may be noted that our data do not contradict the results of Ref. [9] in the 500-2000 keV neutron energy range. However, at energies above 400 keV the results of Refs [8 and 9] differ significantly in terms of energy dependence, which leads to a factor of 1.4 discrepancy between these data at 600 keV. This shows the need for further refining of the capture cross-section value in this neutron energy range. The results of earlier work on the measurement of capture cross-sections in silver generally agree satisfactorily with the latest data within the limits of measurement errors and allowing for the necessary standardization. The figure shows the evaluation of the capture cross-section

for ^{109}Ag made at the Institute of Physics and Energetics [10], based on the data of Ref. [7] and agreeing well with our data. The other evaluations (ENDF/B-V, JENDL-1, RCN) for silver isotopes were based on the results of earlier work and therefore need to be re-evaluated in the light of the latest measurements.